Mechanistic Studies on Cyclopalladation of the Solvated Palladium(II) Complexes with *N*-Benzyl Triamine Ligands in Various Solvents. Crystal Structures of $[Pd(Sol)(Bn_2Medptn)](BF_4)_2$ (Sol = Acetonitrile and *N*, *N*-Dimethylformamide; $Bn_2Medptn$ = *N*, *N*′-Dibenzyl-4-methyl-4-azaheptane-1,7-diamine) and $[Pd(H_{-1}Bn_2Medptn\text{-}C, N, N', N'')]CF_3SO_3$

Takeyoshi Yagyu, Sen-ichi Aizawa,# and Shigenobu Funahashi*

Laboratory of Analytical Chemistry, Faculty of Science, Nagoya University, Chikusa-ku, Nagoya 464-01

(Received August 29, 1997)

Several solvated palladium(II) complexes with the potentially cyclopalladating dibenzyl ligand have been synthesized. These include $[Pd(CH_3CN)(Bn_2Medptn)](BF_4)_2$ (**1**) ($Bn_2Medptn$ = *N*, *N*′-dibenzyl-4-methyl-4-azaheptane-1,7-diamine), $[Pd(dmf)(Bn_2Medptn)](BF_4)_2$ (**2**) (dmf = *N*, *N*-dimethylformamide), and $[Pd(dmso)(Bn_2Medptn)](BF_4)_2$ (**3**) (dmso = dimethyl sulfoxide), their cyclopalladated complex, $[Pd(H_{-1}Bn_2Medptn\text{-}C, N, N', N'')]CF_3SO_3$ (**4**), the solvated monobenzyl complex, $[Pd(CH_3CN)(BnMedptn)](BF_4)_2$ (**5**) (BnMedptn = *N*-(3-aminopropyl)-*N*′-benzyl-*N*-methyl-1,3-propanediamine), and its deuterated complex, $[Pd(CH_3CN)(BnMedptn\text{-}d_7)](BF_4)_2$ (**6**) ($BnMedptn\text{-}d_7$ = *N*-(3-aminopropyl)-*N*′-heptadeuteriobenzyl-*N*-methyl-1,3-propanediamine). The crystal structures of **1**·CH_3CN·CH_2Cl_2, **2**, and **4** have been determined by X-ray structure analysis to characterize the reactant and the product for the cyclopalladation of the solvated complexes, where one of the *ortho* carbons of **1** is directed toward the palladium(II) center (Pd···C(1) = 3.513(9) Å). The rate constants for the cyclopalladation of **1** at 25 °C in various solvents increase in the order DMF < DMSO≪pyridine, but the reaction does not proceed in acetonitrile or nitromethane. The activation parameters for the cyclopalladation in neat solvent have been obtained as follows: $k^{298} = 5.74\times10^{-6}$ s^{-1}, $\Delta H^{\ddagger} = 104.0\pm1.2$ kJ mol^{-1} and $\Delta S^{\ddagger} = 3.5\pm3.9$ J K^{-1} mol^{-1} for **1** in DMF, $k^{298} = 3.13\times10^{-4}$ s^{-1}, $\Delta H^{\ddagger} = 83.8\pm2.6$ kJ mol^{-1} and $\Delta S^{\ddagger} = -31.0\pm8.8$ J K^{-1} mol^{-1} for **1** in DMSO, $k^{298} = 1.30\times10^{-4}$ s^{-1}, $\Delta H^{\ddagger} = 81.2\pm0.5$ kJ mol^{-1} and $\Delta S^{\ddagger} = -47.0\pm1.8$ J K^{-1} mol^{-1} for **5** in DMF, $k^{298} = 1.76\times10^{-3}$ s^{-1} for **5** in DMSO, $k^{298} = 1.26\times10^{-5}$ s^{-1}, $\Delta H^{\ddagger} = 92.8\pm1.4$ kJ mol^{-1} and $\Delta S^{\ddagger} = -27.5\pm4.4$ J K^{-1} mol^{-1} for **6** in DMF and $k^{298} = 2.69\times10^{-4}$ s^{-1} for **6** in DMSO. The activation enthalpy is reduced as the solvent basicity increases. The kinetic isotope effects (k_H/k_D) for the cyclopalladation of the monobenzyl complex at 25 °C are calculated to be 10.3 in DMF and 6.5 in DMSO using the rate constants for **5** and **6**. It is confirmed from the kinetic results obtained that the nucleophilic attack of the basic solvent on the *ortho* proton is essential for the C–H bond cleavage observed in the activation process. In addition, the fact that the rate constant for the cyclopalladation is proportionally dependent on the concentration of DMSO in nitromethane strongly suggests that the solvent-dissociation pre-equilibrium is negligible in neat basic solvent.

The kinetic properties for the ligand-substitution and solvent-exchange reactions of the square-planar palladium(II) complexes have been extensively studied, and for their reactions an associative mechanism via a trigonal-bipyramidal transition state has been generally accepted.[1,2] On the other hand, a mechanism via the three-coordinate 14-electron intermediate and some other related mechanisms have been claimed for the cyclopalladation which involves C–H bond activation by electrophilic attack of the palladium(II) center.[3—5] However, the dissociation of the ligand from the equatorial plane is enthalpically quite unfavorable because of the large bond energy, and that is the reason why the substitution generally proceeds via activation by the attack of an entering ligand. Accordingly, thorough investigation is required for complete understanding of the incompatibility in the reaction mechanisms, and elucidation of the mechanism for cyclopalladation also gives us further insight into the reactivities of Werner-type palladium(II) complexes because the reactant complexes for the cyclopalladation are often the Werner type. However, there have so far been only a few kinetic studies on the cyclopalladation,[4a,6] although a great number of synthetic studies have been reported.[5a,7]

In order to perform the clear-cut kinetic studies of cyclopalladation it is quite important to follow the simplest reaction system without any side reactions such as polymerization, precipitation, and dissociation of bound ligands. Furthermore, solvent molecules often play important roles in the reaction in solution. Therefore, in this work[8] we have synthesized the solvated palladium(II) complexes with potentially cyclopalladating triamine ligands having a benzyl group at each terminal amine (*N*, *N*′-dibenzyl-4-methyl-4-azaheptane-1,7-diamine, $Bn_2Medptn$) and at one terminal amine (*N*-(3-aminopropyl)-*N*′-ben-

Present address: Faculty of Engineering, Shizuoka University, Johoku, Hamamatsu 432.

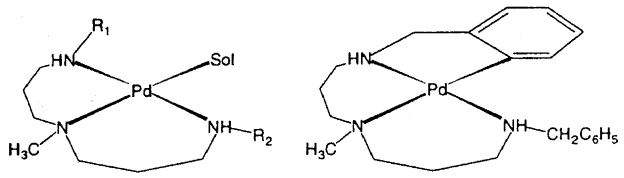

	R_1	R_2	Sol
1	$CH_2C_6H_5$	$CH_2C_6H_5$	CH_3CN
2	$CH_2C_6H_5$	$CH_2C_6H_5$	dmf
3	$CH_2C_6H_5$	$CH_2C_6H_5$	dmso
5	$CH_2C_6H_5$	H	CH_3CN
6	$CD_2C_6D_5$	H	CH_3CN

4

Chart 1.

zyl-*N*-methyl-1,3-propanediamine, BnMedptn). The structural characterization of the solvated dibenzyl complexes, $[Pd(CH_3CN)(Bn_2Medptn)](BF_4)_2$ (**1**) and [Pd(dmf)-$(Bn_2Medptn)](BF_4)_2$ (**2**) (dmf = *N*,*N*-dimethylformamide), and their cyclopalladated complex, $[Pd(H_{-1}Bn_2Medptn\text{-}C, N, N', N'')]CF_3SO_3$ (**4**), has been performed by crystal structure analysis to confirm the structures of the reactants and products in the present cyclopalladation reactions. In order to elucidate the solvent effects on cyclopalladation, the kinetics for **1** in some solvents with different basicity, such as acetonitrile, nitromethane, DMF, dimethyl sulfoxide (DMSO), and pyridine, have been investigated. Furthermore, the role of the basic solvents has been explored by the dependence of the observed rate constant of **1** on the DMSO concentration in nitromethane and the kinetic isotope effects on cyclopalladation in DMF and DMSO using the monobenzyl complex $[Pd(CH_3CN)(BnMedptn)](BF_4)_2$ (**5**) and its deuterated complex $[Pd(CH_3CN)(BnMedptn\text{-}d_7)](BF_4)_2$ (**6**) (BnMedptn-d_7 = *N*-(3-aminopropyl)-*N'*-heptadeuteriobenzyl-*N*-methyl-1,3-propanediamine) (Chart 1). The reaction mechanism of the cyclopalladation is discussed on the basis of the kinetic results.

Experimental

Materials. DMF and DMSO were dried over activated 4A molecular sieves and then purified by distillation under reduced pressure. Acetonitrile and nitromethane were distilled after refluxing for 2 h in the presence of P_2O_5, and pyridine was distilled after refluxing for 2 h in the presence of barium oxide. Deuterated nitromethane and acetonitrile (CD_3NO_2 and CD_3CN, Aldrich) were distilled on a vacuum line after dehydration by activated 4A molecular sieves. The other chemicals were the highest grade commercially available.

Preparation of Ligands. *N*, *N'*-Dibenzyl-4-methyl-4-azaheptane-1,7-diamine (Bn_2Medptn). A solution of *N'*-methyl-3,3'-diaminodipropylamine (30.8 g, 0.212 mol, Wako) and benzaldehyde (52.2 g, 0.492 mol) in ethanol (150 cm^3) was stirred for 22 h at room temperature. The solution to which sodium tetrahydroborate ($NaBH_4$, 37.4 g, 0.989 mol) was added drop by drop was stirred for 20 h at room temperature and then acidified with 12 M HCl (1 M = 1 mol dm^{-3}). The solvent was removed under reduced pressure with a rotary evaporator, and the residue was dissolved in water. The solution was alkalified with aqueous NaOH, and the resultant oily product was extracted with toluene. After evaporation of the solvent, triamine trihydrochloride dihydrate was crystallized from aqueous HCl. Yield: 55.6%. Anal. Found: C, 53.43; H, 8.06; N, 8.81%. Calcd for $C_{21}H_{34}Cl_3N_3\cdot 2H_2O$: C, 53.56; H, 8.13; N, 8.92%.

The crystals of Bn_2Medptn·3HCl·$2H_2O$ were dissolved in water. The solution was alkalified with aqueous NaOH, followed by extraction of the free amine with toluene, and then the toluene solution was dried with anhydrous Na_2SO_4 for 1 d, followed by filtration. The colorless oil of Bn_2Medptn was obtained from the filtrate by evaporation of the solvent. Yield: 75%. ^{1}H NMR ($CDCl_3$) δ = 1.5 (s, 2 H, NH), 1.7 (quin, 4 H, $CH_2CH_2CH_2$), 2.2 (s, 3H, NCH_3), 2.4 (t, 4 H, CH_2NCH_3), 2.6 (t, 4 H, CH_2NBn), 3.8 (s, 4 H, CH_2Ph), 7.2—7.3 (m, 10 H, Ph).

***N*-(3-Aminopropyl)-*N'*-benzyl-*N*-methyl-1,3-propanediamine (BnMedptn).** A solution of *N'*-methyl-3,3'-diaminodipropylamine (94.1 g, 0.648 mol, Wako) and benzyl chloride (30.6 g, 0.242 mol) in ethanol (200 cm^3) was stirred for 60 h at room temperature. Then an aqueous solution (30 cm^3) of NaOH (10.2 g, 0.255 mol) was added. The solution was stirred for 7 h at room temperature. The solvent and the remaining reactants were removed under reduced pressure, and then an excess of aqueous NaOH was added to the residue. The resulting oily product was extracted with toluene. The toluene solution was dried with anhydrous Na_2SO_4 for 1 d followed by filtration. After the solvent was evaporated from the filtrate, 5.63 g of the residue was chromatographed on an SiO_2 column by elution with a $CHCl_3$/methanol/concd aqueous NH_3 (10 : 4 : 1) solution. The eluate was examined by thin-layer chromatography. The appropriate fractions were combined and the solvent was removed to obtain BnMedptn. Yield: 22.5%. ^{1}H NMR ($CDCl_3$) δ = 1.4 (s, 3 H, NH and NH_2), 1.6 (quin, 2 H, $CH_2CH_2CH_2$NBn), 1.7 (quin, 2 H, $CH_2CH_2CH_2NH_2$), 2.2 (s, 3 H, NCH_3), 2.4 (m, 4 H, CH_2NCH_3), 2.7 (t, 2 H, CH_2NBn), 2.7 (t, 2 H, CH_2NH_2), 3.8 (s, 2 H, CH_2Ph), 7.2—7.3 (m, 5 H, Ph).

***N*-(3-Aminopropyl)-*N'*-heptadeuteriobenzyl-*N*-methyl-1,3-propanediamine (BnMedptn-d_7).** A solution of *N'*-methyl-3,3'-diaminodipropylamine (9.36 g, 64.4 mmol, Wako) and benzyl chloride-d_7 (2.92 g, 21.9 mmol, Aldrich) in ethanol (150 cm^3) was stirred for 4 d at room temperature. The solution to which was added an aqueous solution (10 cm^3) of NaOH (1.01 g, 25.3 mmol) was stirred for 16 h at room temperature. After removal of the solvent and the remaining reactants under reduced pressure, excess aqueous NaOH was added to the residue. The resultant oily product was extracted to the $CHCl_3$ phase, which was dried with anhydrous Na_2SO_4. The concentrated filtrate was chromatographed on an SiO_2 column by the same procedure as for BnMedptn to obtain BnMedptn-d_7. Yield: 31.3%. ^{1}H NMR ($CDCl_3$) δ = 1.6 (quin, 2 H, $CH_2CH_2CH_2$NBn-d_7), 1.7 (quin, 2 H, $CH_2CH_2CH_2NH_2$), 1.9 (s, 3 H, NH and NH_2), 2.2 (s, 3 H, NCH_3), 2.4 (m, 4 H, CH_2NCH_3), 2.7 (t, 2 H, CH_2NBn-d_7), 2.7 (t, 2 H, CH_2NH_2).

Preparation of Complexes. $[Pd(CH_3CN)(Bn_2Medptn)](BF_4)_2$ (1). A solution of $[Pd(CH_3CN)_4](BF_4)_2$ (1.32 g, 2.70 mmol, Aldrich, 91%) and Bn_2Medptn (0.978 g, 3.00 mmol) in acetonitrile (30 cm^3) was stirred for 3 h at room temperature. The solution was filtered and the filtrate was concentrated under reduced pressure. To the solution was added dichloromethane to give light yellow crystals. Yield: 91.5%. Anal. Found: C, 42.54; H, 5.20; N, 8.67%. Calcd for $C_{23}H_{34}B_2F_8N_4Pd$: C, 42.73; H, 5.30; N, 8.67%. ^{1}H NMR (CD_3NO_2) δ = 2.0—3.2 (m, $(CH_2)_3$), 2.3 (s, CH_3CN), 3.1 (s, NCH_3), 4.0 and 4.3 (q, CH_2Ph), 4.7 (s(br), NH), 7.5—7.6 (m, Ph). Single crystals of the acetonitrile complex (**1**) were obtained by recrystallization from an acetonitrile–dichloromethane solution.

[Pd(dmf)(Bn$_2$Medptn)](BF$_4$)$_2$ (2). 208 mg (0.322 mmol) of the acetonitrile complex (**1**) was dissolved in DMF (1 cm^3) and the solution was kept at room temperature for 5 min. To the solution was added CH_2Cl_2 (5 cm^3). This was followed by filtration, and to the filtrate was added diethyl ether. The resulting light yellow powder was filtered under nitrogen and dried under vacuum. Yield: 90.7%. Anal. Found: C, 42.46; H, 5.68; N, 8.23%. Calcd for $C_{24}H_{38}B_2F_8N_4OPd$: C, 42.54; H, 5.50; N, 8.27%. ^{1}H NMR (CD_3NO_2) δ = 1.9—3.2 (m, $(CH_2)_3$), 2.8 and 3.1 (s, CH_3 of dmf), 3.0 (s, NCH_3), 3.9 and 4.3 (q, CH_2Ph), 4.0 (s(br), NH), 7.4—7.7 (m, Ph), 7.9 (s, CH of dmf). The single crystals of the dmf complex (**2**) were obtained by crystallization of **1** from a DMF–dichloromethane–diethylether solution.

[Pd(dmso)(Bn$_2$Medptn)](BF$_4$)$_2$ (3). A solution of the acetonitrile complex (**1**) (90 mg, 0.14 mmol) and DMSO (1 cm^3) in nitromethane (30 cm^3) was stirred for 2 min. To the solution was added diethyl ether. The resulting light yellow powder was filtered and washed with ether under nitrogen and dried under vacuum. Yield: 75%. Anal. Found: C, 41.31; H, 5.86; N, 6.66%. Calcd for $C_{23}H_{37}B_2F_8N_3OPdS$: C, 40.41; H, 5.46; N, 6.15%. ^{1}H NMR (CD_3NO_2) δ = 2.0—3.2 (m, $(CH_2)_3$), 2.8 (s, CH_3 of dmso), 3.0 (s, NCH_3), 4.0 (q, CH_2Ph), 3.8 (s(br), NH), 7.5—7.6 (m, Ph). The pure complex was not obtained because the cyclopalladation proceeded simultaneously during the above procedure.

[Pd(H$_{-1}$Bn$_2$Medptn-*C*,*N*,*N*′,*N*″)]CF$_3$SO$_3$ (4). To a solution of Bn$_2$Medptn (0.815 g, 2.50 mmol) in acetonitrile (20 cm^3) was added a solution of $K_2[PdCl_4]$ (0.796 g, 2.44 mmol) in a water/acetonitrile (5 : 4 v/v) mixture (45 cm^3) with stirring. After the solvent was removed by evaporation, water (40 cm^3) was added to the residue. The resultant light yellow precipitate was filtered and dried under vacuum. [PdCl(Bn$_2$Medptn)]Cl·2H$_2$O was obtained. Yield: 75.7%. Anal. Found: C, 47.03; H, 6.58; N, 7.72%. Calcd for $C_{21}H_{31}N_3Cl_2Pd$·2H$_2$O: C, 46.81; H, 6.55; N, 7.80%.

An excess of $AgCF_3SO_3$ (1.9 g, 7.4 mmol) was added to a suspension of [PdCl(Bn$_2$Medptn)]Cl·2H$_2$O (0.995 g, 1.85 mmol) in water (100 cm^3). The resultant precipitate of AgCl was filtered off. The filtrate adjusted to ca. pH 7 by adding aqueous NaOH was stirred for 2 h with boiling and subsequently cooled. The resultant precipitate of the cyclopalladated complex was filtered. The white powder was obtained by recrystallization from a methanol–water solution and then dried under vacuum. Yield: 70.0%. Anal. Found: C, 45.97; H, 5.33; N, 7.21%. Calcd for $C_{22}H_{30}F_3N_3O_3PdS$: C, 45.56; H, 5.21; N, 7.25%. ^{1}H NMR (DMF-d_7) δ = 1.6—3.1 (m, $(CH_2)_3$), 2.9 (s, NCH_3), 4.1 (m, CH_2Ph (pendant)), 4.5 (m, CH_2Ph (bound)), 5.4 and 6.1 (NH), 7.0—7.7 (m, Ph). Single crystals of **4** were obtained by recrystallization from a methane solution.

[Pd(CH$_3$CN)(BnMedptn)](BF$_4$)$_2$ (5). A solution of [Pd(CH$_3$CN)$_4$](BF$_4$)$_2$ (3.42 g, 7.01 mmol, Aldrich, 91%) and BnMedptn (1.77 g, 7.52 mmol) in acetonitrile (50 cm^3) was stirred for 0.5 h at room temperature, followed by filtration. The filtrate was concentrated and chromatographed on a Sephadex LH-20 column by elution with acetonitrile. The eluate was examined spectrophotometrically and the appropriate fractions containing the acetonitrile complex with the monobenzyl ligand were combined. The resultant light yellow powder obtained by addition of diethylether was filtered and dried under vacuum. Yield: 17.5%. Anal. Found: C, 34.82; H, 5.17; N, 9.68%. Calcd for $C_{16}H_{28}B_2F_8N_4Pd$: C, 34.54; H, 5.07; N, 10.07%. ^{1}H NMR (CD_3NO_2) δ=2.0—3.4 (m, $(CH_2)_3$), 2.3 (s, CH_3CN), 2.9 (s, NCH_3), 3.8 and 4.4 (q, CH_2Ph), 3.8 and 4.8 (s(br), NH and NH_2), 7.5—7.8 (m, Ph).

[Pd(CH$_3$CN)(BnMedptn-d_7)](BF$_4$)$_2$ (6). The acetonitrile complex with a deuterated benzyl group was prepared by the same procedure as for **4** using BnMedptn-d_7 instead of BnMedptn. Yield: 29.4%. ^{1}H NMR (CD_3NO_2) δ = 2.0—3.4 (m, $(CH_2)_3$), 2.3 (s, CH_3CN), 2.9 (s, NCH_3), 3.8 and 4.8 (s(br), NH and NH_2).

X-Ray Structure Determination. Each single crystal of **1**, **2**, and **4** suitable for diffraction measurements was sealed in a 0.7-mm or 0.5-mm o.d. thin-wall capillary because the crystals are deliquescent. The X-ray diffraction measurements were performed on a MAC Science Rapid X-Ray Diffraction Image Processor (DIP 320N) with graphite-monochromated Mo $K\alpha$ radiation. Reflections were collected using 30 continuous Weissenberg photographs with a ϕ range of 6° (total ϕ range, 0—180°). The intensity data were corrected for the standard Lorentz and polarization effects. No empirical absorption correction was applied. The structures were solved by the direct method and refined by the full-matrix least-squares technique using Crystan-G (ver. 3).[9] All non-hydrogen atoms were refined with anisotropic thermal parameters, and the hydrogen atoms were placed in the observed positions with fixed thermal parameters. No enantiomer check was carried out for **1** and **2**. Atomic scattering factors and anomalous dispersion terms were taken from Ref. 10. The crystallographic data are summarized in Table 1. The atomic coordinates and thermal parameters of the hydrogen atoms, the anisotropic thermal parameters of the non-hydrogen atoms, bond distances and angles, and $F_o - F_c$ tables have been deposited as Document No. 71010 at the Office of the Editor of Bull. Chem. Soc. Jpn.

Sample Preparations and Measurements. Sample preparations for NMR measurements were carried out in a glovebox or on a vacuum line by distilling the purified solvent on the complex in 5 mm o.d. NMR tubes that were then flame-sealed to avoid contamination with water. ^{1}H NMR measurements were performed on a Bruker AMX-400WB NMR spectrometer operating at 400.13 MHz.

The samples for the kinetic measurements of the cyclopalladation of **1**, **5**, and **6** in DMF, DMSO, and pyridine were prepared on a vacuum line by a procedure similar to that for the NMR measurements using in a vacuum line twice-fused quartz cuvettes that were then flame-sealed. The samples for the dependence of the rate constant on the DMSO concentration of **1** in nitromethane were prepared using the cuvettes separable from a vacuum line in order to weigh nitromethane and DMSO added stepwise. The kinetic measurements at various temperatures were performed with a Shimadzu UV-265FW spectrophotometer. The temperature of the reaction solution was held constant within ±0.1 K. The reactions were followed by a change in absorbance at 296 nm and 304 nm for **1** in DMF and DMSO, respectively, at 283 nm for **5** and **6** in DMF, at 292 nm for **5** and **6** in DMSO and at 390 nm for the dependence of the rate constants on DMSO concentration for **1** in nitromethane. The rate constants were determined by a least-squares analysis for several half-lives.

Results and Discussion

Crystal Structure. The perspective views of **1**, **2**, and **4** are displayed in Figs. 1, 2, and 3, respectively, along with the atomic numbering schemes. The complexes have a square-planar geometry. The crystal of the acetonitrile complex (**1**) contains one acetonitrile and one dichloromethane as solvent of crystallization in each formula unit as represented by [Pd(CH$_3$CN)(Bn$_2$Medptn)](BF$_4$)$_2$·CH$_3$CN·CH$_2$Cl$_2$. The crystal of the dmf complex (**2**) consists of two nonequivalent formula units. Lists of fractional atomic coordinates and isotropic thermal parameters are given in Table 2 for

Table 1. Crystallographic Data for $\mathbf{1}\cdot CH_3CN\cdot CH_2Cl_2$, **2**, and **4**

	$\mathbf{1}\cdot CH_3CN\cdot CH_2Cl_2$	**2**	**4**
Formula	$PdCl_2F_8N_5C_{26}B_2H_{39}$	$PdF_8ON_4C_{24}B_2H_{38}$	$PdSF_3O_3N_3C_{22}H_{30}$
Fw	772.6	678.6	580.0
Size of cryst./mm	$0.60\times0.30\times0.25$	$0.52\times0.40\times0.32$	$0.28\times0.22\times0.12$
Space group	*Pn*	*Pn*	$P\bar{1}$
a/Å	12.138(2)	21.173(4)	9.581(2)
b/Å	13.152(3)	13.096(2)	10.556(2)
c/Å	10.797(2)	10.826(2)	13.394(3)
α/°			102.64(1)
β/°	104.38(2)	102.07(1)	109.39(2)
γ/°			102.13(1)
V/Å^3	1669.6(6)	2935.6(9)	1186.6(5)
Z	2	4	2
T/K	293	293	293
λ/Å	0.71073	0.71073	0.71073
ρ_c/g cm^{-3}	1.537	1.536	1.623
No. of reflections measured	11699	16043	7974
No. of unique reflections	3226	5906	4451
No. of reflections used	3226	5906	4451
No. of variables	489	810	386
μ/cm^{-1}	7.02	6.25	8.25
R[a)]	0.053	0.073	0.071
R_w[b)]	0.054	0.092	0.080
S	1.79	2.40	2.00

a) $R=\sum||F_o|-|F_c||/\sum|F_o|$. b) $R_w=[\sum w(|F_o|-|F_c|)^2/\sum w|F_o|^2]^{1/2}$.

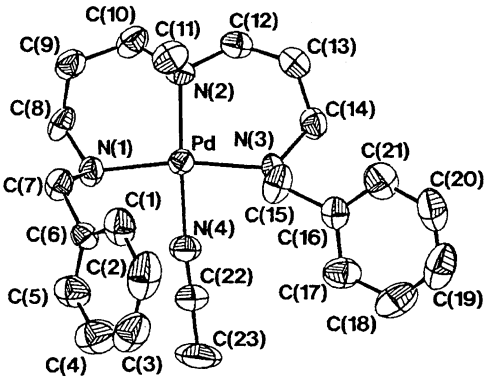

Fig. 1. ORTEP diagram of $[Pd(CH_3CN)(Bn_2Medptn)](BF_4)_2\cdot CH_3CN\cdot CH_2Cl_2$ ($\mathbf{1}\cdot CH_3CN\cdot CH_2Cl_2$) with ellipsoids at 50% probability. All hydrogen atoms, crystallizing CH_3CN and CH_2Cl_2, and BF_4^- counter anions have been omitted for clarity.

$\mathbf{1}\cdot CH_3CN\cdot CH_2Cl_2$, in Table 3 for **2**, and in Table 4 for **4**. The selected bond distances and angles are summarized in Tables 5 and 6, respectively.

The bond distances between palladium(II) and amine nitrogen atoms for **1** are slightly longer than the corresponding bond distances for the acetonitrile complex with 3,3′-diaminodipropylamine (dptn), $[Pd(CH_3CN)(dptn)](CF_3SO_3)_2$ (2.045(1) and 2.036(5) Å for the terminal nitrogens and 2.039(6) Å for the central nitrogen).[11] Such elongation of the bonds for **1** is due to the electron-withdrawing benzyl groups on the terminal amine nitrogens and the slightly lower basicity of the tertiary amine group of $Bn_2Medptn$ compared with the secondary amine group of dptn. No significant difference in the coordination structure around the Pd(II) center is observed between **1** and **2**, except for the difference in the coordinated solvent (CH_3CN for **1** and dmf for **2**). The six-membered chelate rings of the $Bn_2Medptn$ ligand are obviously too large to form the regular square-planar geometry with the palladium(II) ion. Consequently, the chelate bite angles (93.7(3)—98.5(7)°) are much greater than 90° (see Table 6). It should be noted that there is a difference in the orientation of the benzyl groups between **1** and **2**. The *ortho* carbon in one benzyl group of **1** is directed toward the palladium(II) center (Pd···C(1) = 3.513(9) Å) (see Fig. 1), while both benzyl groups of **2** are oriented outside (see Fig. 2). The difference in stability between the two types of orientation of the benzyl group is regarded as almost negligible, based on the fact that the Pd···C(1) distance in **1** is relatively long and the rotation of the benzyl group is not hindered. One set of the NMR signals of the methylene protons of benzyl groups shows that the benzyl groups rotate rapidly in solution. It is plausible that the orientations of the benzyl groups as observed in crystal structures coexist in solution. The orientation of the benzyl group as in **1** may be required to initiate the cyclopalladation but that is not sufficient to promote the cyclopalladation; this is apparent because the cyclopalladation did not proceed in an acetonitrile-dichloromethane solution for the crystallization of **1** but did in a DMF–dichloromethane–diethylether solution for the crystallization of **2** (see Experimental Section). The crystal structures relative to the cyclopalladation, such as $[PdI_2\{2\text{-}I\text{-}C_6H_4(CH_2N(Me)CH_2CH_2NMe_2)\text{-}2\}]$,[4b] bis(azobenzene)dichloropalladium(II),[12] and bis(benzylidenemethylamine)dichloropalladium(II),[13] have been reported. The interaction

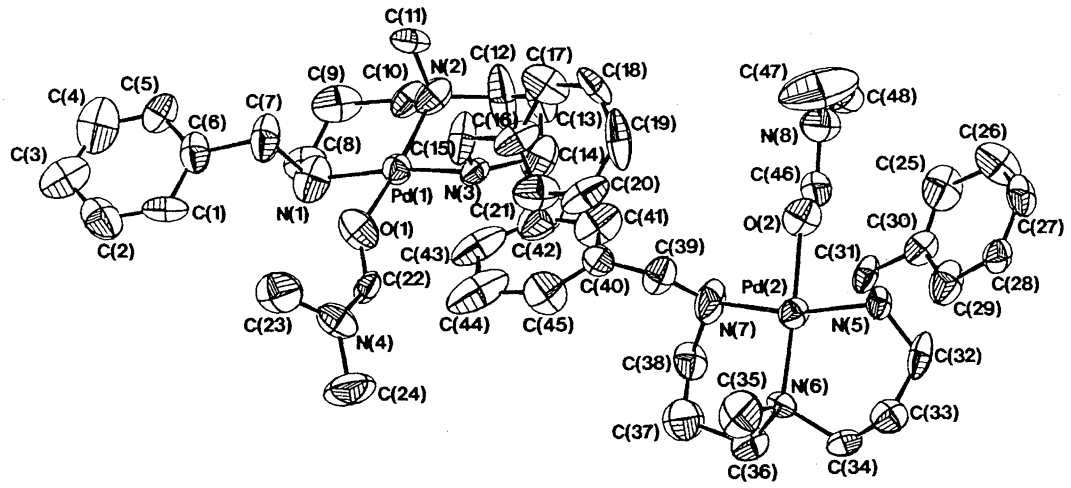

Fig. 2. ORTEP diagram of [Pd(dmf)(Bn_2Medptn)](BF_4)$_2$ (**2**) with ellipsoids at 50% probability. All hydrogen atoms and BF_4^- counter anions have been omitted for clarity.

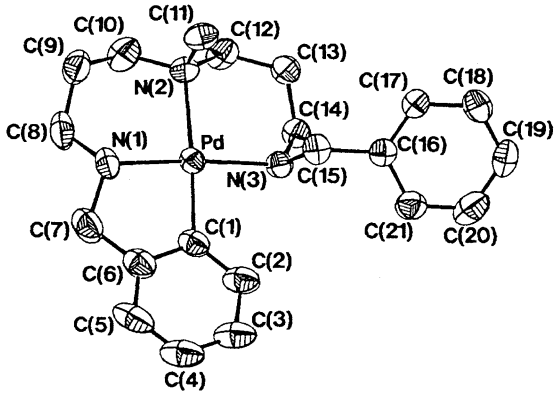

Fig. 3. ORTEP diagram of [Pd($H_{-1}Bn_2$Medptn-*C*, *N*, *N*′, *N*″)]CF_3SO_3 (**4**) with ellipsoids at 50% probability. All hydrogen atoms and $CF_3SO_3^-$ counter anion have been omitted for clarity.

between the *ortho* carbon and the palladium atom is assisted by the electrostatic interaction between the *ortho* proton and the halo ligand. However, such an additional interaction has not been observed in **1**. The crystal structure for **2** appears to be the first instance of a reactant complex obtained in the reaction solution where the cyclopalladation is proceeding.

The cyclopalladated complex (**4**) has large chelate bite angles for the six-membered chelate rings (N(1)–Pd–N(2) = 92.8(2)° and N(2)–Pd–N(3) = 93.1(2)°), as also seen in the acetonitrile and dmf complexes (**1** and **2**) and a small chelate bite angle for the five-membered chelate ring (C(1)–Pd–N(1)=82.4(2)°). The bond distances for the terminal nitrogens (N(1) and N(3)) are in the same range as those for **1** and **2**, while the bond for the central nitrogen (N(2)) is appreciably elongated because of the *trans* influence of the strong Pd–C σ bond. It should be pointed out that the absolute configuration of the terminal amine nitrogen may become inverse with the cyclopalladation. Complexes **1** and **2** in the crystal take *meso* forms where the terminal amine nitrogens have *R* and *S* configuration with axially oriented benzyl groups, while the two terminal amine nitrogens take the same absolute configuration in the crystal of **4**. These configurational changes with cyclopalladation reduce the strain of the tetradentate ligand in complex **4**.

Solvent Effect. The ^{1}H NMR spectrum for the solution of **1** in DMF-d_7 for the freshly prepared solution is shown in Fig. S1a as supporting data. We can assign the singlet at 3.1 ppm to the *N*-methyl protons, the singlet at 5.4 ppm to the amine protons of both terminals, the multiplet around 4.2 ppm to the methylene protons of the pendant benzyl groups, the multiplets in the range of 1.9—3.2 ppm to the methylene protons of the six-membered chelate rings, and the multiplets in the range of 7.4—7.7 ppm to the phenyl protons. The singlet at 2.1 ppm corresponds to the peak for free acetonitrile in the bulk.[14] The absence of the signal for the coordinated acetonitrile indicates that the substitution of the coordinated acetonitrile by DMF-d_7 in the bulk is rapid enough to complete the reaction during the preparation of the sample. The ^{1}H NMR spectrum was changed gradually with time, and the spectrum after the termination of the reaction (Fig. S1b) showed essentially the same spectrum as the cyclopalladated complex (**4**) in DMF-d_7 (see Experimental). The observed rate constants obtained from the increase in the intensity of the new signals for the methylene (4.5 ppm), amine (6.0 ppm), and phenyl (7.0 ppm) protons were in agreement with those determined spectrophotometrically.

It has been confirmed by the ^{1}H NMR measurements that the cyclopalladation of the acetonitrile complex (**1**) does not proceed in acetonitrile or nitromethane, but does proceed in DMSO and pyridine. It should be noted that the presence of a small amount of water in acetonitrile or nitromethane brings about the cyclopalladation, because water acts as a base (see Experimental). The reaction rate in each solvent is substantially different in the order: pyridine≫DMSO > DMF. Accordingly, a more basic solvent[15] is more favorable for the cyclopalladation.

The kinetics of the cyclopalladation was investigated spectrophotometrically. The flame-sealed samples in which water was completely removed were used; otherwise the isosbestic points were not observed in the spectral change, probably

Table 2. Atomic Coordinates and Equivalent Isotropic Thermal Parameter for **1**·CH_3CN·CH_2Cl_2

Atom	x	y	z	B_{eq}/Å^2
Pd	0.25609	0.28610(2)	0.03097	2.78(1)
Cl1	0.3523(6)	0.7354(6)	0.725(1)	12.4(2)
Cl2	0.3578(5)	0.9006(6)	0.5515(9)	12.6(2)
F1	0.353(1)	0.474(1)	0.758(1)	11.5(5)
F2	0.454(2)	0.389(2)	0.641(2)	17.6(8)
F3	0.2720(9)	0.419(1)	0.558(1)	11.1(5)
F4	0.406(1)	0.526(1)	0.580(1)	13.4(6)
F5	0.0703(9)	0.976(1)	0.592(1)	10.3(4)
F6	0.044(1)	0.8878(8)	0.410(1)	11.0(4)
F7	−0.0961(5)	0.9870(6)	0.4473(8)	7.2(2)
F8	0.0610(7)	1.0564(6)	0.4104(9)	7.7(2)
N1	0.2270(4)	0.4277(3)	−0.0577(6)	3.2(1)
N2	0.2598(4)	0.3379(4)	0.2127(7)	3.5(1)
N3	0.2665(4)	0.1321(4)	0.0857(7)	3.2(2)
N4	0.2652(6)	0.2339(6)	−0.1403(8)	3.9(2)
N5	0.536(2)	0.345(1)	0.138(2)	10.2(6)
C1	−0.0264(7)	0.3004(6)	−0.152(1)	4.8(3)
C2	−0.081(1)	0.2223(6)	−0.233(2)	6.8(5)
C3	−0.067(1)	0.2146(7)	−0.360(2)	7.0(6)
C4	−0.005(1)	0.2836(9)	−0.394(2)	6.7(5)
C5	0.0525(6)	0.3603(7)	−0.317(1)	4.9(3)
C6	0.0426(5)	0.3677(4)	−0.1968(9)	3.4(2)
C7	0.1024(5)	0.4508(5)	−0.1099(9)	3.8(2)
C8	0.2841(5)	0.5147(4)	0.0188(9)	4.0(2)
C9	0.2573(6)	0.5271(5)	0.1457(9)	4.1(2)
C10	0.3076(6)	0.4437(6)	0.238(1)	4.3(2)
C11	0.1425(7)	0.3395(7)	0.232(1)	4.8(2)
C12	0.3381(9)	0.2739(7)	0.312(1)	4.2(3)
C13	0.3097(8)	0.1622(6)	0.317(1)	4.5(2)
C14	0.3362(6)	0.1027(5)	0.2080(9)	4.0(2)
C15	0.1465(5)	0.0933(4)	0.055(1)	4.5(2)
C16	0.1373(5)	−0.0199(4)	0.0390(8)	3.5(2)
C17	0.1388(7)	−0.0631(6)	−0.076(1)	4.8(2)
C18	0.1276(8)	−0.1697(8)	−0.092(1)	5.9(3)
C19	0.110(1)	−0.2267(7)	0.009(2)	6.3(4)
C20	0.1076(8)	−0.1836(7)	0.116(1)	5.8(3)
C21	0.1219(8)	−0.0807(7)	0.137(1)	5.2(3)
C22	0.2758(8)	0.1984(7)	−0.235(1)	4.4(3)
C23	0.285(2)	0.157(1)	−0.350(2)	7.3(5)
C24	0.576(1)	0.3470(9)	0.052(2)	6.5(4)
C25	0.629(2)	0.346(1)	−0.053(2)	8.4(5)
C26	0.315(1)	0.859(1)	0.687(2)	9.0(6)
B1	0.3730(9)	0.4516(9)	0.639(2)	6.3(4)
B2	0.0195(7)	0.9758(8)	0.460(1)	5.0(3)

due to side reactions.[16] The change in the spectrum for **1** in DMF as a function of reaction time is shown in Fig. 4, as one instance, exhibiting isosbestic points at 283 and 317 nm. Almost the same spectral change occurred in DMSO, having isosbestic points at 292 and 323 nm, while the reaction in pyridine was completed during the sample preparation.[17] The spectra after the termination of the reaction in DMF, DMSO, and pyridine are identical with those of the cyclopalladated complex (**4**) in the respective solvents. The observed first-order rate constants are independent of the concentration of **1** in DMF (Table 7). Though the solvated palladium(II) complexes consist of one palladium(II) cation and two BF_4^- anions in solid, the free anion exists in the sample solution, because of the incomplete formation of the 1 : 2 ion-pair species.[18] Thus, the observed first-order rate constants would depend on the concentration of **1**, if the counter anion could contribute to the cyclopalladation, due to the ion-pair formation and/or the nucleophilic attack on the *ortho* proton. Consequently, the cyclopalladation proceeds quantitatively without the influence of the counter anion under the present experimental conditions. The temperature dependence of the first-order rate constants, k, was fitted to the Eyring equation to give the values of activation enthalpy ($\Delta H^{\ddagger}$) and activation entropy ($\Delta S^{\ddagger}$) for the cyclopalladation of **1** in DMF and DMSO (Fig. 5 and Table 8).

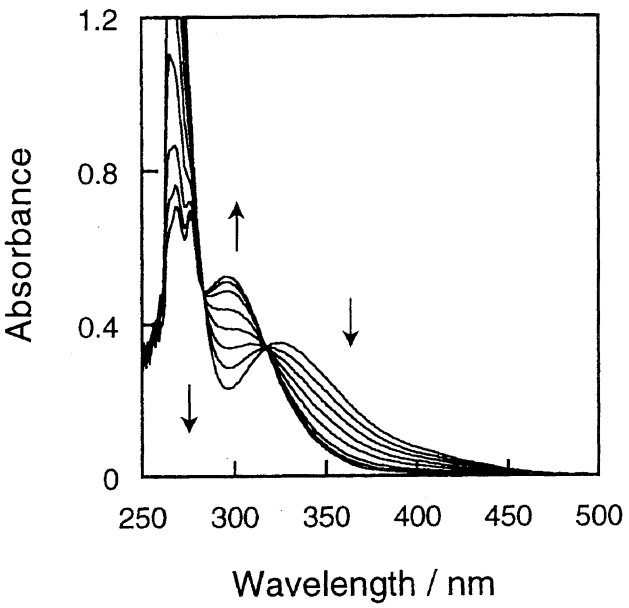

Fig. 4. Absorption spectral changes of **1** in DMF at 341.9 K and $[\mathbf{1}] = 4.97 \times 10^{-4}$ mol kg^{-1}. The spectra were recorded at 0, 60, 130, 220, 350, 570, 820 and 1295 min after the temperature equilibration.

The rate constants at 25 °C in various solvents are in the order pyridine ≫DMSO > DMF, but the reaction does not proceed in acetonitrile or nitromethane, which corresponds to the order of the basicity[15] of the solvents. The difference in rates is mainly attributed to the difference in the activation enthalpy. The present results suggest that the nucleophilic attack of the basic solvent on the *ortho* proton is included in the activation process for cyclopalladation. This suggestion is confirmed by the DMSO concentration dependence of the rate constant and the kinetic isotope effect dependent on the solvent, as described below.

DMSO Concentration Dependence of the Rate. While the cyclopalladation does not proceed in nitromethane as described above, it has been found that cyclopalladation does occur in the presence of DMSO in nitromethane. In order to clarify the role of the solvent as a base in the activation state in further detail, we have investigated the dependence of the observed rate constant of **1** on the DMSO concentration in nitromethane. Because this reaction system is also moisture-sensitive, the samples were prepared using a vacuum line for exclusion of water (see Experimental). As shown in Fig. 6,

Table 3. Atomic Coordinates and Equivalent Isotropic Thermal Parameters for **2**

Atom	x	y	z	B_{eq}/Å^2	Atom	x	y	z	B_{eq}/Å^2
Pd1	−0.00587	−0.00340(4)	0.17398	3.54(3)	C13	0.0401(7)	−0.060(1)	−0.100(1)	6.5(4)
Pd2	0.24471(3)	−0.50357(4)	−0.0369(1)	3.53(4)	C14	0.0933(6)	−0.0640(9)	0.017(1)	5.9(4)
F1	−0.2006(6)	−0.306(1)	−0.001(1)	12.6(4)	C15	0.0980(6)	0.1094(9)	0.100(2)	6.5(5)
F2	−0.2131(9)	−0.311(2)	0.193(1)	14.8(6)	C16	0.1622(5)	0.1251(6)	0.063(1)	4.9(3)
F3	−0.2982(6)	−0.322(1)	0.044(3)	22(1)	C17	0.1682(6)	0.1722(8)	−0.048(1)	5.4(3)
F4	−0.235(1)	−0.438(1)	0.066(3)	20(1)	C18	0.2258(6)	0.184(1)	−0.080(1)	5.2(3)
F5	0.0672(5)	0.368(1)	−0.186(1)	11.9(4)	C19	0.2791(6)	0.147(1)	−0.009(2)	7.6(5)
F6	0.0010(8)	0.335(1)	−0.352(1)	12.2(5)	C20	0.2783(6)	0.115(1)	0.114(2)	6.7(4)
F7	−0.0421(5)	0.377(1)	−0.205(2)	16.0(7)	C21	0.2179(6)	0.101(1)	0.143(1)	6.0(4)
F8	0.0063(6)	0.2357(8)	−0.184(1)	11.2(4)	C22	0.0815(5)	0.0110(6)	0.429(1)	3.6(3)
F9	0.0401(8)	−0.181(2)	−0.386(1)	15.1(6)	C23	0.0812(9)	0.158(1)	0.560(2)	7.2(4)
F10	−0.0273(7)	−0.0568(7)	−0.445(2)	12.8(5)	C24	0.156(1)	0.008(1)	0.636(3)	8.2(7)
F11	−0.0518(8)	−0.2037(7)	−0.361(1)	11.3(5)	C25	0.3622(6)	−0.3624(9)	−0.346(2)	6.4(4)
F12	−0.036(1)	−0.206(2)	−0.545(2)	19(1)	C26	0.4045(6)	−0.349(1)	−0.434(1)	6.4(4)
F13	0.2744(6)	−0.1070(9)	0.326(1)	10.2(4)	C27	0.4672(6)	−0.3339(8)	−0.387(1)	5.1(3)
F14	0.2280(4)	−0.2679(7)	0.321(1)	9.0(3)	C28	0.4945(4)	−0.3411(7)	−0.254(1)	4.0(2)
F15	0.1721(4)	−0.1238(7)	0.294(1)	8.6(3)	C29	0.4538(6)	−0.3632(9)	−0.169(1)	6.1(4)
F16	0.2384(6)	−0.1654(7)	0.491(1)	9.7(4)	C30	0.3886(4)	−0.3762(6)	−0.219(1)	3.9(2)
O1	0.0427(5)	0.0515(7)	0.3393(9)	5.7(2)	C31	0.3466(5)	−0.3923(6)	−0.130(1)	4.0(3)
O2	0.1974(3)	−0.4457(5)	−0.2066(8)	4.6(2)	C32	0.3739(4)	−0.5714(7)	−0.081(1)	5.0(3)
N1	−0.081(1)	0.0017(6)	0.264(3)	6.2(6)	C33	0.4027(5)	−0.5630(7)	0.062(1)	4.5(3)
N2	−0.0594(4)	−0.0439(6)	−0.009(1)	4.8(3)	C34	0.3588(6)	−0.602(1)	0.135(1)	6.4(4)
N3	0.0811(5)	0.0042(4)	0.119(1)	3.3(3)	C35	0.3203(8)	−0.440(1)	0.218(2)	7.4(5)
N4	0.1070(4)	0.0554(8)	0.5319(9)	4.9(2)	C36	0.2621(6)	−0.6043(9)	0.212(1)	5.5(3)
N5	0.3249(6)	−0.4996(4)	−0.123(2)	3.2(3)	C37	0.1957(7)	−0.563(1)	0.233(2)	7.0(5)
N6	0.2970(4)	−0.5377(9)	0.1340(9)	4.0(2)	C38	0.1453(5)	−0.5693(8)	0.114(1)	4.7(3)
N7	0.152(1)	−0.4982(7)	0.010(2)	7.0(7)	C39	0.1401(5)	−0.3861(8)	0.038(1)	4.7(3)
N8	0.1317(4)	−0.4426(8)	−0.397(1)	5.2(3)	C40	0.0716(5)	−0.3712(8)	0.064(1)	4.5(3)
C1	−0.1269(6)	0.1349(7)	0.486(1)	4.9(3)	C41	0.0169(6)	−0.4079(9)	−0.016(2)	6.4(4)
C2	−0.1684(8)	0.1598(9)	0.564(1)	7.1(4)	C42	−0.0433(6)	−0.400(1)	0.019(2)	7.4(5)
C3	−0.2380(8)	0.171(1)	0.518(2)	7.0(5)	C43	−0.0473(7)	−0.345(1)	0.140(2)	7.5(5)
C4	−0.256(1)	0.164(1)	0.389(2)	8.0(7)	C44	0.012(1)	−0.313(2)	0.238(3)	10.8(8)
C5	−0.2160(4)	0.1453(7)	0.310(1)	4.5(2)	C45	0.0703(6)	−0.331(1)	0.182(1)	6.1(4)
C6	−0.1513(5)	0.1310(8)	0.352(1)	4.9(3)	C46	0.1566(9)	−0.496(1)	−0.289(2)	6.8(6)
C7	−0.1026(7)	0.1132(9)	0.261(2)	6.3(4)	C47	0.151(1)	−0.347(2)	−0.433(3)	12.7(9)
C8	−0.1422(6)	−0.0677(8)	0.216(1)	5.0(3)	C48	0.0896(8)	−0.501(1)	−0.490(3)	7.3(7)
C9	−0.1637(5)	−0.0641(9)	0.077(1)	6.0(3)	B1	−0.2405(7)	−0.3426(9)	0.073(2)	7.0(5)
C10	−0.1171(5)	−0.1035(6)	−0.003(1)	4.8(3)	B2	0.0136(7)	0.335(1)	−0.223(1)	5.0(3)
C11	−0.0777(4)	0.0554(9)	−0.063(1)	4.3(3)	B3	−0.0236(7)	−0.164(1)	−0.441(1)	5.9(4)
C12	−0.0235(7)	−0.103(1)	−0.083(2)	8.9(5)	B4	0.2308(5)	−0.173(1)	0.367(1)	4.8(3)

the rate constant is almost proportional to the concentration of DMSO in the bulk at 301.4, 310.3, and 314.9 K, within the experimental errors.

The three-coordinate species without the bound solvent have not been observed in the ^{1}H NMR spectra for the dmf complex (**2**) and the dmso complex (**3**) in nitromethane-d_3.[19] Consequently, we can regard the existence of the three-coordinate species formed by the solvent-dissociation pre-equilibrium as negligible in the initial state in the case of the present kinetic measurements, because neat DMF or DMSO was used as the solvent. The absence of such a pre-equilibrium is supported by the linearity of the plots of the DMSO concentration dependence of the observed rate constant (Fig. 6). Furthermore, if the solvent-dissociation path is operative in the cyclopalladation where the intermediate is quite reactive and the steady-state approximation can be applied, the observed rate constants are expected to be independent of the DMSO concentration. Even if one may expect that a slight intercept is concealed by the experimental errors, the solvent-dissociation path becomes more negligible in a neat basic solvent. Furthermore, though the relationship as shown in Fig. 6 also corresponds to the mechanism where another solvent binds to the axial site and the bound solvent abstracts the *ortho* proton, we can rule out this mechanism on the basis of the following reasons; the five coordinate palladium(II) complex is so bulky that the electrophilic attack of the palladium(II) center on the *ortho* carbon is sterically difficult, and the five coordinate 18-electron species is electronically saturated and does not allow the electrophilic attack of the palladium(II) center. Accordingly, we reasonably conclude that the present cyclopalladation proceeds via the nucleophilic attack of the basic solvent in the bulk on the *ortho* proton of

Table 4. Atomic Coordinates and Equivalent Isotropic Thermal Parameters for **4**

Atom	x	y	z	B_{eq}/Å^2
Pd	0.31584(3)	0.37028(3)	−0.21591(3)	3.12(2)
S	0.1604(2)	0.0188(1)	0.2750(1)	4.37(4)
F1	0.121(1)	0.1345(9)	0.1199(7)	13.8(4)
F2	0.3352(9)	0.2297(5)	0.2589(6)	12.7(3)
F3	0.3035(7)	0.0462(5)	0.1432(5)	9.5(2)
O1	0.0898(5)	0.1052(4)	0.3240(4)	5.9(2)
O2	0.2992(7)	0.0066(6)	0.3525(5)	7.5(2)
O3	0.0555(6)	−0.1074(4)	0.1921(4)	6.3(2)
N1	0.2652(6)	0.2766(4)	−0.1076(4)	4.0(1)
N2	0.3492(5)	0.1878(4)	−0.3100(4)	3.5(1)
N3	0.3442(5)	0.4769(4)	−0.3244(4)	3.5(1)
C1	0.2689(6)	0.5233(5)	−0.1281(5)	3.8(1)
C2	0.2458(8)	0.6409(6)	−0.1527(6)	5.1(2)
C3	0.2004(8)	0.7311(6)	−0.0864(7)	6.0(2)
C4	0.1762(8)	0.7064(6)	0.0028(6)	6.3(2)
C5	0.1980(8)	0.5905(7)	0.0282(6)	5.8(2)
C6	0.2464(7)	0.5008(5)	−0.0360(5)	4.4(2)
C7	0.2799(9)	0.3797(6)	−0.0057(6)	5.6(2)
C8	0.346(1)	0.1796(8)	−0.0742(6)	5.8(2)
C9	0.3260(9)	0.0628(6)	−0.1732(6)	5.5(2)
C10	0.4125(8)	0.1061(7)	−0.2399(7)	5.5(2)
C11	0.1916(7)	0.1043(5)	−0.3959(6)	4.5(2)
C12	0.4586(7)	0.2181(6)	−0.3642(6)	5.0(2)
C13	0.4313(7)	0.3127(5)	−0.4343(5)	4.4(2)
C14	0.4645(6)	0.4568(5)	−0.3672(5)	3.8(2)
C15	0.1904(5)	0.4518(5)	−0.4135(5)	3.7(1)
C16	0.1887(5)	0.5269(4)	−0.4977(5)	3.5(1)
C17	0.1485(6)	0.4567(4)	−0.6072(4)	3.8(1)
C18	0.1339(6)	0.5228(6)	−0.6877(5)	4.4(2)
C19	0.1636(7)	0.6615(6)	−0.6569(6)	5.2(2)
C20	0.2083(8)	0.7342(6)	−0.5474(7)	6.0(2)
C21	0.2197(7)	06680(5)	−0.4686(5)	4.7(2)
C22	0.2343(9)	0.1118(6)	0.1960(7)	5.8(2)

Table 5. Selected Bond Distances (Å) for **1**·CH_3CN·CH_2Cl_2, **2**, and **4**

		1·CH_3CN·CH_2Cl_2			
Pd–N1	2.084(5)	Pd–N2	2.067(7)	Pd–N3	2.105(5)
Pd–N4	2.001(9)	Pd···C1	3.513(9)		
		2			
Pd1–N1	2.02(3)	Pd1–N2	2.13(1)	Pd1–N3	2.05(1)
Pd1–O1	2.002(9)	Pd2–N5	2.10(2)	Pd2–N6	1.999(9)
Pd2–N7	2.12(2)	Pd2–O2	2.045(7)		
		4			
Pd–C1	2.005(6)	Pd–N1	2.053(6)	Pd–N2	2.206(4)
Pd–N3	2.074(5)				

the four-coordinate solvated complex.

Kinetic Isotope Effects. We consider that the *ortho* C–H bond cleavage plays a significant role in the activation process for the cyclopalladation, judging from the quite large values of $\Delta H^{\ddagger}$ for **1** in DMF and DMSO and the dependence of the rate on the solvent basicity. Consequently, we have confirmed the magnitude of the kinetic isotope effects (k_H/k_D) in DMF and DMSO using the monobenzyl complex (**5**) and

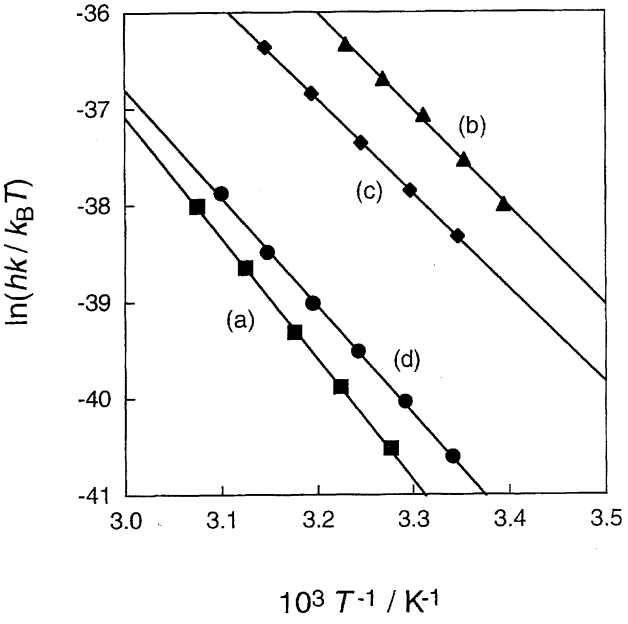

Fig. 5. Temperature dependence of the rate constants k for cyclopalladation of **1** in DMF ([**1**] = (2.71—10.3)×10^{-4} mol kg^{-1}) (a), **1** in DMSO ([**1**] = (3.82—6.31)×10^{-4} mol kg^{-1}) (b), **5** in DMF ([**5**] = (4.41—6.94)×10^{-4} mol kg^{-1} (c), and **6** in DMF ([**6**] = (4.54—6.43)×10^{-4} mol kg^{-1}) (d).

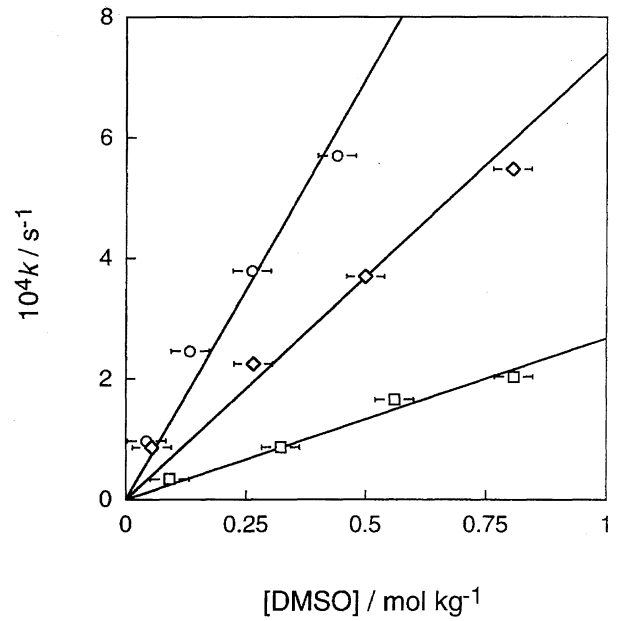

Fig. 6. The dependence of the rate constants on DMSO concentration of cyclopalladation of **1** in nitromethane at 301.4 K ([**1**] = 1.62—1.97)×10^{-3} mol kg^{-1}) (□), at 310.3 K ([**1**] = (1.13—1.73)×10^{-3} mol kg^{-1}) (◇) and at 314.9 K ([**1**] = (1.85—2.20)×10^{-3} mol kg^{-1}) (○). Considering the precision of the present sample preparation, the upper limit of the experimental errors in the DMSO concentration is ca. 0.04 mol kg^{-1}, which corresponds to each bar.

Table 6. Selected Bond Angles (deg) for **1**·CH_3CN·CH_2Cl_2, **2**, and **4**

		1·CH_3CN·CH_2Cl_2			
N1–Pd–N2	95.9(2)	Pd–N1–C8	115.6(4)	C10–N2–C12	104.0(6)
N1–Pd–N3	168.7(2)	C7–N1–C8	109.9(4)	C11–N2–C12	111.5(8)
N1–Pd–N4	85.6(3)	Pd–N2–C10	113.2(6)	Pd–N3–C14	119.9(4)
N2–Pd–N3	93.7(3)	Pd–N2–C11	110.0(6)	Pd–N3–C15	106.1(4)
N2–Pd–N4	175.7(2)	Pd–N2–C12	110.6(6)	C14–N3–C15	115.6(7)
N3–Pd–N4	85.2(3)	C10–N2–C11	107.4(6)	Pd–N4–C22	175.0(7)
Pd–N1–C7	113.0(4)				
		2			
N1–Pd1–N2	98.0(8)	Pd1–N1–C8	120(2)	Pd2–N5–C32	117(1)
N1–Pd1–N3	167.6(8)	C7–N1–C8	108(1)	C31–N5–C32	116(1)
N1–Pd1–O1	82.3(8)	Pd1–N2–C10	112.0(8)	Pd2–N6–C34	115.4(7)
N2–Pd1–N3	94.4(4)	Pd1–N2–C11	101.3(6)	Pd2–N6–C35	113.2(8)
N2–Pd1–O1	173.3(3)	Pd1–N2–C12	114.3(7)	Pd2–N6–C36	113.8(6)
N3–Pd1–O1	85.3(4)	C10–N2–C11	110.0(7)	C34–N6–C35	105.8(9)
N5–Pd2–N6	94.1(5)	C10–N2–C12	106(1)	C34–N6–C36	101.2(9)
N5–Pd2–N7	167.3(8)	C11–N2–C12	113(1)	C35–N6–C36	106(1)
N5–Pd2–O2	83.3(5)	Pd1–N3–C14	119.6(7)	Pd2–N7–C38	114(1)
N6–Pd2–N7	98.5(7)	Pd1–N3–C15	110.6(8)	Pd2–N7–C39	106(1)
N6–Pd2–O2	170.8(4)	C14–N3–C15	112(1)	C38–N7–C39	113(2)
N7–Pd2–O2	84.1(7)	C22–N4–C23	118.6(9)	C46–N8–C47	127(1)
Pd1–O1–C22	132.2(8)	C22–N4–C24	125(1)	C46–N8–C48	114(1)
Pd2–O2–C46	124.3(9)	C23–N4–C24	116(1)	C47–N8–C48	118(2)
Pd1–N1–C7	107(1)	Pd2–N5–C31	109.6(9)		
		4			
C1–Pd–N1	82.4(2)	Pd–N1–C8	119.2(5)	C11–N2–C12	110.0(5)
C1–Pd–N2	174.2(2)	C7–N1–C8	109.1(5)	Pd–N3–C14	115.6(4)
C1–Pd–N3	91.3(2)	Pd–N2–C10	113.2(4)	Pd–N3–C15	109.1(4)
N1–Pd–N2	92.8(2)	Pd–N2–C11	105.4(4)	C14–N3–C15	113.5(5)
N1–Pd–N3	172.4(2)	Pd–N2–C12	114.1(3)	Pd–C1–C2	128.6(5)
N2–Pd–N3	93.1(2)	C10–N2–C11	109.4(4)	Pd–C1–C6	113.6(4)
Pd–N1–C7	110.6(4)	C10–N2–C12	104.7(5)		

Table 7. Observed Rate Constants at Various Concentrations of the Palladium(II) Complex for Cyclopalladation of **1** in DMF at 314.9 K

[Pd complex]/10^{-4} mol kg^{-1}	10^5 k_{obs}/s^{-1}
2.71	5.51
4.97	5.76
6.95	5.38
10.3	5.52

Table 8. Activation Parameters and Rate Constants at 25 °C for Cyclopalladation of Palladium(II) Complexes in DMF and DMSO

Complex[a)]	Solvent	$\Delta H^{\ddagger}$/kJ mol^{-1}	$\Delta S^{\ddagger}$/J K^{-1} mol^{-1}	$10^6 k^{298}$/s^{-1}
1	DMF	104.0±1.2	3.5±3.9	5.74
5	DMF	81.2±0.5	-47.0±1.8	130
6	DMF	92.8±1.4	-27.5±4.4	12.6
1	DMSO	83.8±2.6	-31.0±8.8	313
5	DMSO			1760
6	DMSO			269

a) See text; **1**: dibenzyl complex, **5**: monobenzyl complex, **6**: deuterated monobenzyl complex.

the deuterated monobenzyl complex (**6**) because the rate for the deuterated dibenzyl complex is expected to be unfavorably slow for the kinetic measurements. Spectral changes similar to those for **1** in DMF and DMSO were observed in the cases of both **5** and **6**, exhibiting isosbestic points at 266 and 313 nm in DMF and at 276 and 312 nm in DMSO, respectively, though the rate for the monobenzyl complex (**5**) was distinctly faster than that for the dibenzyl complex (**1**) and appreciable retardation of the reaction of the deuterated monobenzyl complex (**6**) compared with that of **5** was observed. The temperature dependence of the rate constants for **5** and **6** in DMF is shown in Fig. 5, and the activation parameters obtained in DMF and the rate constants observed at 25 °C in DMSO are listed in Table 8, together with those for the dibenzyl complex (**1**) in DMF and DMSO.

The kinetic isotope effects (k_H/k_D) at 25 °C for the monobenzyl complex are 10.3 and 6.5 in DMF and DMSO, respectively. These values are extremely large compared with those reported for other cyclopalladation reactions.[4a,6b] The large kinetic isotope effect[20] in DMF comes from the large difference in the activation enthalpy such as 11.6 kJ mol^{-1} (see Table 8), and presumably includes the tunnel effect. Consequently, it is reasonable that the energy required for the C–H bond cleavage on the *ortho* carbon of the benzyl group

is mainly reflected in the activation energy observed, though the electrophilic attack of the palladium(II) center on the *ortho* carbon[21] and the nucleophilic attack of the basic solvent on the *ortho* proton described above also make a contribution to the activation of the *ortho* C–H bond cleavage. The nucleophilic attack of the basic solvent is also supported by the smaller kinetic isotope effect in DMSO than that in DMF. The stronger base, DMSO, is more advantageous for nucleophilic attraction toward the *ortho* proton, which induces a relatively greater inverse kinetic isotope effect by a contribution of the bond formation between the *ortho* proton and the solvent molecule. Actually, a relatively small value of the kinetic isotope effect (k_H/k_D =1.5) was reported for the cyclopalladation of the bis(acetylacetonato)palladium(II) complex with 2-phenylpyridine in *n*-butanol,[6b] where an excess of 2-phenylpyridine act as the strong base for the nucleophilic attraction. Considering that such an interaction between the *ortho* proton and the basic solvent reduces the energy for the C–H bond cleavage, we think it is reasonable that the order of magnitude of the kinetic isotope effect (DMF > DMSO) agrees with that of the activation enthalpy.

In the present work, the steric effect on the cyclopalladation has also been observed. As is apparent from Table 8, the rate constants at 25 °C for **5** are much greater than those for **1** in DMF and DMSO. Taking into account the electron-withdrawing properties of the benzyl group, the dibenzyl complex (**1**) is more advantageous for the electrophilic attack of the palladium(II) center than the monobenzyl complex (**5**). However, the reaction of **5** is enthalpically more favorable than that of **1** as shown for the reaction in DMF. It is most probable that the pendant benzyl group in the dibenzyl complex (**1**) has a repulsive interaction with the approaching solvent and/or benzyl group keeping those away from the reaction site on the palladium(II) center. Such blocking of the pendant benzyl group may weaken the interaction between the approaching solvent and the leaving *ortho* proton and/or between the *ortho* carbon and the palladium(II) center in the transition state to give a large value of $\Delta H^{\ddagger}$ and a less negative value of $\Delta S^{\ddagger}$. Thus, the steric hindrance around the reaction site is one of the significant factors which influence the reactivity of cyclopalladating complexes.

Conclusions

We have confirmed the structures of the reactants and products for the cyclopalladation and have accomplished mechanistic studies under the conditions without contamination with water. The main conclusions drawn are as follows.

The cyclopalladation proceeds via the electrophilic attack of the palladium(II) center on the *ortho* carbon of the benzyl group, which is directed toward the palladium(II) center as observed in the crystal structure of **1**. In the transition state, the nucleophilic attack of the basic solvent molecule on the *ortho* proton is essential to cleavage the *ortho* C–H bond, as clarified by the kinetic isotope effect and the kinetic properties dependent on the solvent. It has been confirmed that acetonitrile does not have sufficient basicity to promote the cyclopalladation, while the activation energy for the C–H bond cleavage is reduced as the basicity of the solvent increases, as observed in DMF, DMSO, and pyridine. In addition, the solvent-dissociation pre-equilibrium is not expected from the proportionality of the dependence of the rate constant on the concentration of the basic solvent in the bulk. In our present reaction systems, we can rule out the mechanism via the three-coordinate 14-electron intermediate as claimed previously.

Supporting Data. Crystallographic materials (Tables S1—S16) and ^{1}H NMR spectra of **1** in deuterated DMF at 315.5 K, just after preparation and after 22 h (Fig. S1) are deposited as Document No. 71010 at the Office of the Editor of Bull. Chem. Soc. Jpn. and are also available from the author on request.

This work has been supported by Grants-in-Aid for Scientific Research Nos. 07454199 and 07504003 from the Ministry of Education, Science, Sports and Culture. S. A. gratefully acknowledges financial support by a grant from the Kurata Foundation. We thank Mr. Toshiaki Noda for his efforts in constructing the vacuum distiller for the high boiling solvents.

References

1) R. G. Wilkins, "Kinetics and Mechanism of Reactions of Transition Metal Complexes," 2nd ed, VCH, Weinheim (1991), Chap. 4; R. J. Cross, "Mechanisms of Inorganic and Organometallic Reactions," ed by M. V. Twigg, Plenum, New York (1988), Chap. 5, and references therein.

2) L. Helm, L. I. Elding, and A. E. Merbach, *Helv. Chim. Acta*, **67**, 1453 (1984); B. Brøunnum, H. S. Johansen, and L. H. Skibsted, *Acta Chem. Scand.*, **43**, 975 (1989); J. Berger, M. Kotowski, R. van Eldik, U. Frey, L. Helm, and A. E. Merbach, *Inorg. Chem.*, **28**, 3759 (1989); N. Hallinan, V. Besançon, M. Forster, G. Elbaze, Y. Ducommun, and A. E. Merbach, *Inorg. Chem.*, **30**, 1112 (1991); U. Frey, S. Elmroth, B. Moullet, L. I. Elding, and A. E. Merbach, *Inorg. Chem.*, **30**, 5033 (1991); Y. Ducommun, L. Helm, A. E. Merbach, B. Hellquist, and L. I. Elding, *Inorg. Chem.*, **28**, 377 (1989).

3) A. J. Deeming and I. P. Rothwell, *Pure Appl. Chem.*, **52**, 649 (1980); A. J. Deeming and I. P. Rothwell, *J. Organomet. Chem.*, **205**, 117 (1981).

4) a) A. D. Ryabov, I. K. Sakodinskaya, and A. K. Yatsimirsky, *J. Chem. Soc., Dalton Trans.*, **1985**, 2629; b) P. L. Alsters, P. F. Engel, M. P. Hogerheide, M. Copijn, A. L. Spek, and G. van Koten, *Organometallics*, **12**, 1831 (1993); 2-I-$C_6H_4(CH_2N(Me)$-$CH_2CH_2NMe_2)$-2 = *N*-(2-iodobenzyl)-*N*,*N*′,*N*′-trimethylethane-1, 2-diamine: c) J. Vicente, I. Saura-Llamas, and P. G. Jones, *J. Chem. Soc., Dalton Trans.*, **1993**, 3619; d) J.-M. Valk, F. Maassarani, P. van der Sluis, A. L. Spek, J. Boersma, and G. van Koten, *Organometallics*, **13**, 2320 (1994); e) A. J. Canty and G. van Koten, *Acc. Chem. Res.*, **28**, 406 (1995).

5) a) V. V. Dunina, O. A. Zalevskaya, and V. M. Potapov, *Russ. Chem. Rev.*, **57**, 250 (1988); b) A. D. Ryabov, *Chem. Rev.*, **90**, 403 (1990), and references therein.

6) a) A. D. Ryabov, *Inorg. Chem.*, **26**, 1252 (1987); b) R. P. Thummel and Y. Jahng, *J. Org. Chem.*, **52**, 73 (1987).

7) I. Omae, *Chem. Rev.*, **79**, 287 (1979); G. R. Newkome, W. E.

Puckett, V. K. Gupta, and G. E. Kiefer, *Chem. Rev.*, **86**, 451 (1986), and references therein.

8) T. Yagyu, S. Aizawa, and S. Funahashi, *Chem. Lett.*, **1996**, 1107.

9) "Programmes of Structure Determination Package," MAC Science, Yokohama (1992).

10) "International Tables for X-Ray Crystallography," Kynoch Press, Birmingham (1974), Vol. 4.

11) T. Yagyu, S. Aizawa, K. Hatano, and S. Funahashi, *Bull. Chem. Soc. Jpn.*, **69**, 1961 (1996).

12) G. P. Khare, R. G. Little, J. T. Veal, and R. J. Doedens, *Inorg. Chem.*, **14**, 2475 (1975).

13) L. G. Kuz'mina and Yu. T. Struchkov, *Cryst. Struct. Commun.*, **8**, 715 (1979).

14) The coordinated acetonitrile of **1** in deuterated nitromethane shows a singlet at 2.3 ppm as described in Experimental section.

15) W. C. Barrette, Jr., H. W. Johnson, Jr., and D. T. Sawyer, *Anal. Chem.*, **56**, 1890 (1984).

16) This side reaction may come from decomposition of palladium(II) complexes due to the hydrolysis of DMF or DMSO.

17) The reaction was complete within 30 s in the preliminary measurements using a quartz cuvette with a Teflon® cap.

18) The analogous palladium(II) complex, $[Pd(CH_3CN)(diethylenetriamine)](BF_4)_2$, forms the 1 : 1 ion pair quantitatively at $C_{BF_4^-} = 0.8$ mol kg^{-1} in nitromethane as shown in Ref. 11, where $C_{BF_4^-}$ is the total concentration of BF_4^-.

19) The judgment for complex **2** is conveniently made by the signals of the formyl proton at 7.91 ppm for the bound DMF and at 7.82 ppm for the free DMF because there is no overlapping peak in this region. Furthermore, no change in the chemical shifts of the bound solvent was observed over the temperature range from −33 to 60 °C. Similarly, no signal for the methyl protons at 2.5 ppm for the free DMSO but at 2.8 ppm for the bound DMSO was observed in the ^{1}H NMR spectrum for **3**.

20) L. Melander, "Isotope Effects on Reaction Rates," Ronald, New York (1960); J. Bigeleisen, *J. Chem. Phys.*, **17**, 675 (1949); R. P. Bell, *Chem. Soc. Rev.*, **3**, 513 (1974).

21) It is expected that the electrophilic attack by the non-bonding empty $5p_z$ orbital is operative as is general with the associative mechanism for the Pd(II) complexes.